Published in final edited form as:
Arthritis Rheum. 2009 November ; 60(11): 3324–3335. doi:10.1002/art.24877.

A novel secreted osteoclastogenic factor of activated T cells (SOFAT) induces osteoclast formation in a RANKL-independent manner

Leonard Rifas, M.S.[1] and **M. Neale Weitzmann, Ph.D.**[2,3,4]

[1] Department Of Pediatrics, Washington University School Of Medicine, St. Louis, Missouri

[2] Division of Endocrinology & Metabolism & Lipids, Department of Medicine, Emory University School of Medicine, Atlanta, Georgia

[3] Winship Cancer Institute, Emory University School of Medicine, Atlanta, Georgia

[4] Atlanta Veterans Affairs Medical Center, Atlanta, Georgia 30033

Abstract

Objective—Chronic T cell activation is central to the etiology of rheumatoid arthritis (RA) an inflammatory autoimmune disease that leads to severe focal bone erosions and generalized systemic osteoporosis. We previously reported novel cytokine-like activities in media from activated T cells that potently induced osteoblastic IL-6 production, an inflammatory cytokine and stimulator of osteoclastogenesis, as well as an activity that directly stimulated osteoclast formation independently of the key osteoclastogenic cytokine receptor activator of NF-κB ligand (RANKL). In this study we sought to identify the factor(s) secreted by T cells that are responsible for these activities.

Methods—T cells were activated using anti-human CD3 and anti-human CD28 antibodies for 72 Hr in Aim V serum free medium and T cell conditioned media (C.M.) concentrated, and fractionated by fast protein liquid chromatography (FPLC). Biologically active fractions were resolved on SDS-PAGE and major bands subjected to mass-spectrometry (MS). A major candidate protein was identified, cloned and expressed using recombinant DNA technologies.

Results—We identified a single novel cytokine inducing both osteoblastic IL-6 production, and functional osteoclast formation, in the absence of osteoblasts or RANKL, and in an OPG-insensitive manner. We named this cytokine secreted osteoclastogenic factor of activated T cells (SOFAT). SOFAT is derived from an unusual mRNA splice-variant coded by the threonine synthase-like 2 (THNSL2) gene homolog, a conserved gene remnant coding for threonine synthase, an enzyme that only functions in microorganisms and plants.

Conclusion—SOFAT may act to exacerbate inflammation and/or bone turnover under inflammatory conditions such as RA, periodontitis and in estrogen deficiency.

RA is a chronic inflammatory disease with complex etiology. Juxta-articular bone loss occurring around inflamed joints, and generalized systemic bone loss are common features of RA [reviewed in (1–3)]. One of the main characteristics of RA is a dense lymphoid infiltration into the synovial membrane.

Corresponding Author/Address for reprint requests: M. Neale Weitzmann, Division of Endocrinology & Metabolism & Lipids, Emory University School of Medicine, 101 Woodruff Circle, 1305 WMRB, Georgia 30322-0001, Tel: (404) 727-1389: Fax (404) 727-1300: MWeitzm@Emory.Edu.

Activated T cells are now considered potent modulators of bone turnover and are a key source of osteoclastogenic cytokines under inflammatory conditions such as RA (4,5) and periodontitis (6,7) and in estrogen deficiency (8–11).

We have recently reported that activated T cells secrete cytokines that potently stimulate the differentiation of human bone marrow stromal cells into osteoblasts (12,13), as well as an unknown factor capable of stimulating IL-6 production by osteoblasts (14). IL-6 is an osteoclastogenic factor that has been implicated in the bone destruction associated with both estrogen deficiency in humans (15–17) and mice (18,19) and in inflammation and osteoporosis in RA (14,16,20).

Activated T cells have also long been known to stimulate osteoclast formation (21–24). T cell derived TNFα production has been reported to play a critical role in ovariectomy induced bone loss in mice (25), and T cell derived RANKL is reported to be relevant in animal models of RA (26). We (27,28) and others (29,30) have reported that activated T cells stimulate osteoclastogenesis in vitro by secretion of RANKL. Interestingly, our data produced the controversial finding that activated T cells also significantly induce osteoclast formation by a mechanism that was independent of RANKL since saturating concentrations of the RANKL inhibitor osteoprotegerin (OPG), failed to neutralize greater than 30% of the observed osteoclast formation induced by activated T cells (28).

Using sequential biochemical purification, mass-spectrometry, and recombinant DNA technologies, we have identified and expressed a novel activated human T cell secreted cytokine, herein referred to as SOFAT. This single cytokine elicits RANKL- and osteoblast-independent osteoclast formation in an OPG-insensitive manner, as well stimulating osteoblast IL-6 production.

Materials and Methods

Materials

Antibodies were from Santa Cruz Biotechnology, (Santa Cruz, CA) unless otherwise indicated. All other reagents were purchased from the Sigma-Aldrich Chemical Co. (St. Louis, MO), unless indicated.

Biochemical purification of SOFAT

T cell C.M. was collected and concentrated using 20 mL Amicon Centricon concentrators (Millipore, Bedford, MA). The concentrate was buffer exchanged to Tris-HCl, pH 8.0 and applied to a DEAE Sepharose column using a FPLC system (Invitrogen, Carlsbad, CA). After washing the column with Tris-HCl, pH 8.0, the column was eluted with a NaCl gradient of 0–1 M. One mL fractions were collected and aliquots were assayed for IL-6 activity using an Endogen ELISA (Pierce Biotechnology, Inc., Rockford, IL) and osteoclast formation resolved by staining the cells for TRAP. The active fractions were then concentrated using a 5,000 da MW cutoff Amicon Centricon concentrator (Millipore) and the concentrated protein buffer exchanged to Tris-Saline, pH 7.4. The protein was applied to a FPLC Superdex-200 gel filtration column in Tris-Saline, pH 7.4. One mL fractions were collected and aliquots assayed for IL-6 activity on human osteoblasts and for osteoclast formation on human monocytes.

SDS-PAGE of SOFAT

Aliquots (5 μg) of purified protein from the DEAE-sephadex or the FPLC Superdex-200 column were diluted 3:1 (vol:vol) with 4x Laemmli sample buffer, boiled for 5 minutes, then separated on a 4–12% Novex Tris-Glycine readymade gel (Invitrogen Corporation).

The gels were then stained with colloidal Coomassie blue stain (Genosystems, Woodlands, TX) according to the manufacturer's instructions.

Mass spectrometry analysis of purified and recombinant human SOFAT (rhSOFAT)

To identify the purified secreted T cell protein, Coomassie blue stained bands were cut out of 10% SDS-Page gels and digested in gel with purified trypsin. The gel was extracted with acetonitrile/trifluoro-acetic acid and subjected to gas chromatography and Matrix-assisted laser desorption (MALDI)/time of flight (TOF) mass spectrometry by the Proteomics Center at Washington University. Recombinant SOFAT was similarly processed and subjected to MALDI/TOF. Peaks were identified using ProteinProspector V5.2.2 (http://prospector.ucsf.edu/).

Cloning of SOFAT

T cells were activated with anti-CD3 and anti-CD28 antibodies in AIM V medium in a 5% CO_2 incubator at 37°C. After 72 hrs total RNA was extracted using a Rneasy kit (Qiagen, Valencia, CA). The isolated RNA was subjected to RT-PCR using a Qiagen one-step RT-PCR kit. Total RNA (1 μg) was subjected to RT for 30 min at 50°C then heated at 95°C for 15 min to destroy the RT enzyme. PCR was conducted at 94°C, 30 sec, 60°C for 30 sec and 72°C for 1 minute for 35 cycles. Primers were reconstructed from the nucleotide sequence encoding a hypothetical threonine-synthase-like protein identified by protein BLAST of Genbank and matching the DNA sequence of FLJ10916 (Accession AK001778). The primers contained flanking *att*B1 and *att*B2 recombination sites to allow for rapid recombination-mediated transfer of SOFAT cDNA from Gateway pDONOR221 plasmid to bacterial (pDEST17) and mammalian (pDEST26) expression plasmids (Invitrogen). These plasmids encode N-terminal 6X histidine tags (His) fused to the recombinant protein to facilitate protein identification and purification. Primer are: forward [5′-GGG GAC AAG TTT GTA CAA AAA AGC AGG CTC CAT GGA CAT TAT CGT TCT GCT GCC C-3′]; and Reverse [5′-GGG GAC CAC TTT GTA CAA GAA AGC TGG GTT CTA CTG GGA GGT GTT GAG GGC ATG-3′] with (SOFAT sequence underlined). We used *E. coli* generated His tagged rhSOFAT for all experiments unless otherwise indicated. pDEST26 was used to express N-terminal His tagged rhSOFAT in CHO cells to investigate secretion of SOFAT in a mammalian system.

Expression of rhSOFAT

The SOFAT cDNA in pDEST17 was used to express a recombinant SOFAT protein in E. coli BL21-A1. After a 3 hr induction with arabinose, bacteria were harvested, lysed and the protein extracted from inclusion bodies, and refolded using the Novagen protein refolding kit according to the manufacturer's protocol. After refolding the protein was further purified on a Qiagen Ni-NTA column according to their provided procedures.

Isolation of T cells

Peripheral blood mononuclear cells (PBMC) were obtained from buffy coats (American Red Cross, St. Louis, MO), and further purified by separation on Histopaque (1.077 gms/mL) lymphocyte separation medium as previously described (31). The use of human buffy coats was approved by the Washington University Institutional Review Board.

Isolation of human Monocytes

$CD14^+$ monocytes were purchased from Stem Cell Technologies (Vancouver, CA) or were isolated from buffy coats using EasySep CD14 Positive Selection Cocktail and EasySep Magnetic Nanoparticles (Stem Cell Technologies, Vancouver, British Columbia, Canada).

Human Osteoclast Formation

Purified human monocytes were plated at a density of 5×10^5 cells/well, in 48-well plates in a final volume of 0.5 respectively of αMEM supplemented with 10% FBS (Hyclone, Logan, UT), penicillin (100 U/mL), streptomycin (100 μg/mL) and 25 ng/mL rhM-CSF (R&D Systems, Minneapolis, MN). Cultures were stimulated with either 10 percent purified T cell SOFAT, doses of rhSOFAT, or with rRANKL (a kind gift of Dr. Beth Lee, Ohio State University). To test for RANKL dependent/independent osteoclast formation cultures were treated with 200× excess OPG (R & D Systems) relative to RANKL. Medium was changed (50 percent) every three to four days for 10 days and stained for tartrate resistant acid phosphatase (TRAP) using a leukocyte acid phosphatase kit.

Murine Osteoclast formation from RAW264.7 Cells

Osteoclasts were generated from the mouse monocytic cell line RAW 264.7 (ATCC Manassas, VA) using rhRANKL (60 ng/mL) and crosslinking anti-6X-His antibody (2.5 μg/mL) (R&D Systems) or with rhSOFAT (100 ng/mL). RAW264.7 cells were seeded into 96 well plates (5–10,000 cells/well) in a final volume of 200 μL of αMEM supplemented with 10% FBS (Hyclone), penicillin (100 U/mL), and streptomycin (100 μg/mL). RAW264.7 cells were cultured at 37°C in a 5% CO_2 incubator for 5–7 days and TRAP stained. In some experiments cultures also received cyclosporine A (CsA) (2 μg/mL), FK506 (10 ng/mL) neutralizing TNFα antibody (20 μg/mL) or IL-6 antibodies (20 μg/mL) from R&D Systems (AF-410-NA and AB-406-NA respectively).. Osteoclasts were quantitated under light microscopy and normalized for number of nuclei. TRAP positive cells with ≥ 3 nuclei were defined as osteoclasts.

Osteoclast Characterization

Immunocytochemistry was performed as previously described (27). Briefly, multinucleated cells were generated with rhSOFAT (100 ng/mL) as described above, fixed for 60 sec with acetone/methanol (50:50, vol/vol) and incubated overnight at 4°C in 3% BSA containing specific mouse or goat anti-human IgG antibodies against αV and β3 integrin subunits, cathepsin K, or the or osteoclast specific antibody 121F, a generous gift of Dr. Philip Osdoby (Washington University, St. Louis, MO). Non-specific binding was assessed by isotype and species (mouse or goat) matched control antibodies as indicated in the figures. After 2 washes in PBS, cells were incubated with secondary antibody (anti-goat or anti-mouse conjugated horseradish peroxidase) for 2 hr at RT. After 3 washes in PBS color was developed using 4-chloronapthol (0.03% in 0.05 M Tris-HCI, pH 7.6, and 0. 1% H_20_2). Actin ring formation was visualized by fluorescence microscopy of cells stained with Phycoerythrin conjugated anti-F actin antibody. Fluorescence and light microscopy was performed on a Nikon Eclipse TE2000-S inverted phase contrast microscope. Images were captured using a digital camera (QImaging Corp., Burnaby, BC, Canada).

Osteoclast activity assays

Resorption was assessed on BD BioCoat Osteologic films (BD Biosciences Franklin Lakes, NJ), an artificial resorbable calcium phosphate film coated onto a quartz substrate. Osteoclasts were cultured directly from RAW264.7 cells on BioCoat using rhSOFAT or rhRANKL. After 10 days, cells were dissociated with 6% bleach for 10 minutes, followed by 3 washes in water. Resorption pits were digitally photographed under bright field and phase contrast microscopy at 200× magnification.

T cell cultures

T cells were cultured at 1×10^6 cells/mL in AIM V serum-free medium (GIBCO). T cells were activated as previously described (13,31) using anti-human CD3 and CD28 antibodies

(Pharmingen). After a 72 hr incubation period at 37°C the activated T cell conditioned medium (C.M.) was harvested and stored at −80°C.

Osteoblast isolation and culture

Human osteoblast cultures were prepared from human ribs as previously described (14,31). Rib specimens were obtained from deceased organ transplant donors through Midwest Transplant Services (St. Louis, MO).

Statistical Analyses

Statistical significance was determined using SigmaStat software (Systat Software, Inc., Richmond, CA). Data represent the mean ± S.E.M. or S.D. as indicated. Group mean values were compared by either One Way ANOVA using the Fisher LSD or Tukey-Kramer post-hoc tests, or the Mann-Whitney test for non-parametric data, as appropriate. $P \leq 0.5$ was considered statistically significant.

Results

Isolation and identification of a novel T cell cytokine with osteoclastogenic and osteoblastic IL-6 inducing activities

In order to identify the factors responsible for osteoblastic IL-6 production and RANKL-independent osteoclast formation activated T cell C.M. was subjected to biochemical fractionation by DEAE-Sepharose anion exchange chromatograph and proteins eluted with a NaCl gradient (Figure 1A). Fractions were assayed for IL-6 induction in human osteoblasts, and for osteoclastogenic activity on human monocyte cultures pre-treated with 25 ng/mL M-CSF (Figure 1A). A major peak of IL-6 inducing activity eluted early in the salt gradient and interestingly, also corresponded to the osteoclastogenic activity as well (Figure 1B). Fractions (21–29) comprising the major peak eluted from the DEAE-Sepharose column (Figure 1A) were pooled and further subjected to Superdex-200 gel filtration chromatography (Figure 1C). The eluted fractions were again assayed for osteoblastic IL-6, and osteoclast inducing activities. A single peak was resolved with an apparent molecular mass of ~27 kDa which induced IL-6 in human osteoblasts (Figure 1C) and again induced osteoclasts when added to purified human monocytes (Figure 1D). The peak IL-6- and osteoclast-inducing fractions from the Superdex S-200 column were again pooled (fractions 32–34) and subjected to SDS-PAGE. A major ~27 kDa product was excised, digested with trypsin and subjected to mass spectrometry. Four peptides were identified and the amino acid sequences used to interrogate the National Center for Biotechnology Information (NCBI) protein database using the Basic Local Alignment Search Tool (BLAST) (32). BLAST analysis revealed strong amino acid sequence homology to Genbank accession number AK001778, (cDNA FLJ10916), a hypothetical protein, based on an open reading frame identified by shotgun genomic cDNA sequencing analysis.

Based on our mass spectroscopy (MS) results and the cDNA sequence reported in FLJ10916 we designed RT-PCR primers (see Methods) and performed RT-PCR on resting and activated T cell total RNA. Activated, but not resting T cells, expressed mRNA for the novel protein as well as for RANKL (Supplemental Figure 1A).

Based on the potent osteoclastogenic activity of this factor we have named it secreted osteoclastogenic factor of activated T cells (SOFAT).

Cloning of SOFAT

The SOFAT cDNA was cloned as described in detail in the Methods section. The full DNA sequence was determined by automated sequencing and found to have a somewhat different

sequence to the previously predicted hypothetical cDNA FLJ10916. The 1002 bp sequence was found to contain a stop codon at nucleotides 742–744 and translated a protein sequence containing 247 amino acids, identical to the natural product isolated biochemically. The amino acid sequence was deduced from SOFAT cDNA using Vector NTI (Invitrogen Corp.) is shown in Figure 2A.

Genomic structure of THNSL2 and mRNA splice variants giving rise to SOFAT

The SOFAT nucleotide sequence was then blasted against the NCBI human genome database, and was found to have significant homology to parts of the THNSL2 gene located on chromosome 2 (2p11.2). THNSL2 is a gene remnant encoding a protein highly similar to threonine synthase, but incapable of l-threonine biosynthesis in vertebrates (33). Bioinformatic analysis using NCBI AceView, Version Human April 07 (http://www.ncbi.nlm.nih.gov/IEB/Research/Acembly/) (34) reveals that the THNSL2 gene contains 26 different introns and that 13 different mRNAs are transcribed. Of these 12 are alternatively spliced variants (designated a to l) and 1 unspliced form (m) (Supplemental Fig. 2). The mRNAs appear to differ based on truncation of the 5′ and/or 3′ ends, the presence or absence of 13 exons, overlapping exons with different boundaries, and alternative splicing or retention of 10 introns. Interestingly, the sequence of SOFAT represents a 14th alternative splice variant with significant, but not complete, homology to variant “b”. SOFAT comprises the last 97 of 153 nucleotides of exon 4, spliced to 231 bp of exon 5, 149 bp of exon 6, 126 bp of exon 7 and 141 bp of exon 8, using THNSL2 splice variant “b” as the reference sequence (Figure 2B). The SOFAT mRNA also contained an additional 33 bp of non-coding 3′ UTR derived from intronic sequence immediately following exon 8, and at least (within the boundaries of our 3′ primer) 258 bp of additional 3′ UTR derived from a ninth exon. Exon 9 is non-coding in both THNSL2 variant “b” and SOFAT, but coding in several other variants (a to l) (see Supplemental Figure 2).

A number of splice variants coded by the THNSL2 gene contain a pyroxidal-5′-phosphate dependent, beta subunit domain, however, SOFAT does not contain the entire domain, suggesting that unlike threonine synthase, SOFAT is not pyroxidal-5′-phosphate dependent.

Our RT-PCR primers have the capacity to identify 7 of the 14 possible variants, (SOFAT, a, b, d, e, f, and g). However, we routinely observed only one major product (SOFAT) in activated T cells, although the region between the primers is the same for SOFAT and variant “b”, and only 19 and 12 bp shorter for variants “a” and “f” respectively. Consequently, they cannot be readily resolved from each other and the extent to which each of these 4 splice isoforms contribute to SOFAT generation remains to be determined (Supplemental Figure 1B).

Recombinant SOFAT Expression

Recombinant SOFAT was expressed from pDEST17 in E. coli BL21-A1 and the resulting His-tagged protein resolved by SDS-PAGE and Western blot using goat anti-polyhistidine antibody (Figure 3A). The protein was found to have a ~27 kDa molecular weight, identical to the natural protein. Mass spectrometry analysis of the purified protein (Figure 3B) revealed a sequence identical to the predicted amino acid translation derived from the cDNA (Figure 2A) confirming the identity of the recombinant protein as SOFAT.

SOFAT was originally identified in T cell conditioned medium however, sequence analysis of SOFAT failed to identify any signal peptide using SignalP 3.0 software for prediction of classically secreted proteins (35,36). In order to verify that SOFAT is secreted by mammalian cells the cDNA for SOFAT was transferred to the mammalian expression vector pDEST26, and recombinant His tagged SOFAT expressed in CHO cells. The conditioned

medium was immunoprecipitated with polyHis antibody and the immunoprecipitated protein subjected to Western Blot and His tag immunoprobing. Empty vector transfected cultures were processed in the same fashion. SOFAT was reproducibly produced and secreted from mammalian cells (Figure 3C). We found no bands from control cultures (Figure 3C, lane 1) or cell lysates from SOFAT expressing cells (data not shown), suggesting that the protein is rapidly secreted.

SOFAT induces IL-6 production by human osteoblasts and osteoclast formation by purified human monocytes

Since the natural form of SOFAT induced IL-6 secretion in human osteoblasts, we tested rhSOFAT) for this activity. rhSOFAT induced IL-6 in human osteoblasts in a dose dependent manner (Figure 3D), confirming that the recombinant protein has the expected biological activity on osteoblasts.

Likewise, we confirmed that rhSOFAT treatment of purified human $CD14^+$ monocytes resulted in the formation of TRAP+ multinuclear cells in a dose dependent fashion (Figure 4A) in the absence of exogenous RANKL or osteoblasts. Doses of rhSOFAT as low as 6 ng/mL stimulated significant osteoclast formation, with maximal production observed at 50 ng/mL.

Osteoclast Characterization

The TRAP+ multinucleated cells generated by rhSOFAT were validated as osteoclasts using multiple specific markers of the osteoclast phenotype including αV and β3 integrin subunit expression, reactivity to the anti-osteoclast antibody 121F (37), cathepsin K, and formation of actin rings (Figure 4B).

SOFAT induces osteoclast formation in a RANKL-independent manner

Since SOFAT induces osteoclastogenesis independently of exogenously added RANKL, we examined whether SOFAT may act by inducing autologous RANKL by human monocytes. When human monocytes were treated with RANKL, osteoclast formation occurred as expected. This process was inhibited by the simultaneous presence of 200 fold excess OPG (Figure 4C). Addition of rhSOFAT to human monocytes likewise induced osteoclast formation but the addition of OPG did not abrogate the effect of SOFAT demonstrating that the mechanism of SOFAT induction of osteoclastogenesis is not mediated by RANKL (Figure 4C).

rhSOFAT induces osteoclast formation in the murine system—Human SOFAT was aligned to human THNSL2 variant “b” as well as to multiple eukaryotic sequences using the BLAST search routine to interrogate the protein sequence database (NCBI) (Supplementary Fig. 3). The THNSL2 amino acid sequence coding for SOFAT is highly conserved across evolution in species as diverse as sea urchin and cow, despite the lack of L-threonine synthesis by this protein (33). Strong homologies between human and other species including other primates such as orangutan (100%) and chimpanzee (98.8%) and a high degree of core homology was observed between human SOFAT and the predicted mouse sequence (87%).

To investigate if, as with most other cytokines, the human cytokine is active in mouse, a model that offers significant advantages in terms of experimental manipulation, we assessed the effect of rhSOFAT on osteoclast formation by RAW264.7 cells. RAW264.7 cells are a well characterized mouse clonal monocytic cell line that generates osteoclasts at high frequency in response to RANKL. rhSOFAT potently induced TRAP+ multinucleated cell formation by RAW264.7 cells (Figure 5A).

SOFAT-Induces functional osteoclasts

To test whether the TRAP+ multinucleated cells generated by rhSOFAT are functional osteoclasts, we seeded RAW264.7 cells on BioCoat Osteologic films, and generated osteoclasts using rhSOFAT or rhRANKL, and photographed resorption pits under bright field and phase contrast microscopy 10 days later. Both RANKL- and SOFAT-induced osteoclasts caused significant pit formation on BioCoat validating these cells as functional osteoclasts (Figure 5B).

Similar to RANKL, rhSOFAT-induced osteoclastogenesis is potently amplified, but not dependent on, TNFα—TNFα is an inflammatory cytokine that is found at high levels in the inflammatory pannus in RA and is central to the etiology of RA. While not stimulating osteoclast formation directly, TNFα has been shown to potently amplify RANKL-induced osteoclast formation (9). Similarly, our data demonstrates that TNFα also potently amplifies SOFAT induced osteoclast formation (Figure 6A and D) although depletion of TNFα from the system by neutralizing antibody failed to prevent osteoclast formation by rhSOFAT (Fig. 6B, D).

rhSOFAT fails to induce IL-6 production by macrophages—IL-6 is another inflammatory cytokine commonly associated with RA, and reported to support osteoclast formation. We have demonstrated that rhSOFAT stimulates potent IL-6 secretion by osteoblasts. To determine whether SOFAT-induced osteoclast formation also involves, in part, direct IL-6 secretion from osteoclast precursors, we added neutralizing IL-6 antibody to rhSOFAT-stimulated osteoclast cultures. IL-6 neutralization failed to impact osteoclast formation by rhSOFAT (Fig. 6C, D). We further stimulated RAW264.7 cells with rhSOFAT for 24 hr and quantitated IL-6 production using a commercial mouse IL-6 specific ELISA. The data show (Supplemental Figure 4), that while LPS potently induced IL-6 secretion, rhSOFAT had no effect, suggesting that SOFAT does not mediate osteoclast formation through autologous production of IL-6 by monocytes.

Finally, RANKL induced c-fos induces NFATc1 synthesis which has been described as a master switch for osteoclastogenesis (38). As with RANKL (Supplemental Figure 5A), SOFAT induced osteoclast formation was sensitive to CsA and FK506, two potent inhibitors of calcineurin, the major upstream regulator of NFATc1 activation (Supplemental Figure 5B). SOFAT signaling, like that of RANKL, thus appears to converge on the NFAT signal transduction pathway. This is consistent with the induction of TRAP, β3-integrin and cathepsin K upregulation by SOFAT, factors reported to have NFATc1 consensus sequences in their gene promoters (39).

Discussion

Threonine synthase is a pyridoxal-5′-phosphate-dependent enzyme that synthesizes L-threonine in plants and microorganisms. However, L-threonine is an essential amino acid as it is not biosynthetically generated in insects, birds and mammals. Interestingly, two homologs (THNSL1 and THNSL2) of threonine synthase, have nonetheless, been conserved throughout evolution and persist in rodents, and mammals including humans (33). The high degree of sequence conservation of threonine synthase genes through evolution is surprising given the apparent lack of L-threonine synthesis in higher organisms. The full-length THNSL2 protein has been reported to bind pyridoxal-5′-phosphate and O-phospho-homoserine degrading them to alpha-ketobutyrate, phosphate, and ammonia; and O-phospho-threonine (PThr) to alpha-ketobutyrate, suggesting catabolic phospho-lyase activity (33). Interestingly, SOFAT does not contain the entire pyridoxal-5′-phosphate binding

domain, suggesting that unlike threonine synthase, SOFAT is not pyroxidal-5′-phosphate dependent.

Our data suggest that a secreted fragment coded by the threonine-synthase homolog may play a critical previously unrecognized function in the immune/skeletal interface. Furthermore, the inappropriate overexpression of this cytokine may drive inflammation and bone destruction in pathological conditions characterized by exuberant T cell activation, such as RA.

We have previously reported that activated T cells produce factors capable of inducing osteoblastic IL-6 production (14) as well as factors that stimulate osteoclastogenesis including RANKL (27,28). However the role of RANKL in inflammatory bone destruction is not clear. RANKL has been implicated in systemic bone destruction in animal models of RA (26). However, patients with RA have elevated serum OPG (40) and the OPG/RANKL ratio tends to be high in the synovium. Furthermore, there is often no correlation with levels of synovial RANKL and disease severity(41). It is thus possible that SOFAT is a critical osteoclastogenic factor in RA.

TNFα has also been found to induce osteoclasts synergistically with RANKL (42) as well as independently of RANKL (43), although these latter effects are controversial. While SOFAT was not found to require TNFα to induce osteoclast formation, it potently amplified osteoclastogenesis. We speculate that the high levels of TNFα present in RA may act to potently magnify SOFAT-induced osteoclastogenesis and bone loss.

In T cells the RANKL gene is regulated by a calcineurin-dependent signaling pathway (44). In contrast, SOFAT is secreted by activated T cells via a calcineurin-independent pathway, as CSA treatment of activated T cells failed to block production of this cytokine (14). Together this suggests that SOFAT production by T cells is stimulated by an intracellular pathway different to that utilized by RANKL, although the specific pathways involved remain to be elucidated.

The role of IL-6 in bone resorption has been primarily associated with post-menopausal osteoporosis, but IL-6 may also play a role in the bone loss seen in RA and other inflammatory arthritides (20). Our data demonstrate that SOFAT fails to stimulate, or augment, osteoclast formation by directly inducing IL-6 secretion by osteoclast precursors. However, IL-6 has been reported to stimulate RANKL-production by synovial fibroblasts derived from RA patients and to mediate TNFα-induced RANKL production in this system (45). IL-6 also functions to induce the proliferation of mononuclear osteoclast precursor cells (46). The demonstration that SOFAT is a potent inducer of IL-6 by osteoblasts suggests that SOFAT could play a significant role in the local inflammatory response, as well exacerbating bone destruction in RA indirectly-through multiple IL-6-mediated events. Interestingly, a new study suggests that IL-6 modulates production of T cell-derived cytokines in antigen-induced arthritis and drives inflammation-induced osteoclastogenesis (47). This data suggests the potential existence of feedback mechanism between activated T cells and osteoblasts, and SOFAT could play a critical role in the coupling of bone cells to the adaptive immune response, thus perpetuating inflammation and osteoclastic bone resorption.

SOFAT may represent the first in a potential family of novel cytokines possessing biological activities in the absence of classical cytokine–like motifs. The pathophysiological functions and mechanisms of action of SOFAT remain to be elucidated.

Supplementary Material

Refer to Web version on PubMed Central for supplementary material.

Acknowledgments

The authors thank Ms. Theresa Geurs for technical assistance, Dr. Henry Rohrs for technical assistance with Mass Spectrometry, and Dr. Philip Osdoby for critical reading of the manuscript.

Grant supporter(s): This work was supported by Grant AR046370 from NIAMS to L. Rifas. M.N. Weitzmann is also supported in part by funding from NIAMS (AR053607 and AR056090), and NCI (CA119338), and the Biomedical Laboratory Research & Development Service of the VA Office of Research and Development (5I01BX000105).

References

1. Deodhar AA, Woolf AD. Bone mass measurement and bone metabolism in rheumatoid arthritis: a review. Br J Rheumatol. 1996; 35(4):309–322. [PubMed: 8624634]
2. Dequeker J, Maenaut K, Verwilghen J, Westhovens R. Osteoporosis in rheumatoid arthritis. Clin Exp Rheumatol. 1995; 13 (Suppl 12):S21–6. [PubMed: 8846540]
3. Gough AK, Peel NF, Eastell R, Holder RL, Lilley J, Emery P. Excretion of pyridinium crosslinks correlates with disease activity and appendicular bone loss in early rheumatoid arthritis. Ann Rheum Dis. 1994; 53(1):14–17. [PubMed: 8311548]
4. Fournier C. Where do T cells stand in rheumatoid arthritis? Joint Bone Spine. 2005; 72(6):527–532. [PubMed: 16087382]
5. Ogawa Y, Ohtsuki M, Uzuki M, Sawai T, Onozawa Y, Nakayama J, et al. Suppression of osteoclastogenesis in rheumatoid arthritis by induction of apoptosis in activated CD4+ T cells. Arthritis Rheum. 2003; 48(12):3350–3358. [PubMed: 14673986]
6. Brunetti G, Colucci S, Pignataro P, Coricciati M, Mori G, Cirulli N, et al. T cells support osteoclastogenesis in an in vitro model derived from human periodontitis patients. J Periodontol. 2005; 76(10):1675–1680. [PubMed: 16253089]
7. Ito H, Honda T, Domon H, Oda T, Okui T, Amanuma R, et al. Gene expression analysis of the CD4+ T-cell clones derived from gingival tissues of periodontitis patients. Oral Microbiol Immunol. 2005; 20(6):382–386. [PubMed: 16238600]
8. Cenci S, Toraldo G, Weitzmann MN, Roggia C, Gao Y, Qian WP, et al. Estrogen deficiency induces bone loss by increasing T cell proliferation and lifespan through IFN-gamma-induced class II transactivator. Proc Natl Acad Sci U S A. 2003; 100(18):10405–10. [PubMed: 12923292]
9. Cenci S, Weitzmann MN, Roggia C, Namba N, Novack D, Woodring J, et al. Estrogen deficiency induces bone loss by enhancing T-cell production of TNF-alpha. J Clin Invest. 2000; 106(10):1229–1237. [PubMed: 11086024]
10. Eghbali-Fatourechi G, Khosla S, Sanyal A, Boyle WJ, Lacey DL, Riggs BL. Role of RANK ligand in mediating increased bone resorption in early postmenopausal women. J Clin Invest. 2003; 111(8):1221–30. [PubMed: 12697741]
11. D'Amelio P, Grimaldi A, Di Bella S, Brianza SZ, Cristofaro MA, Tamone C, et al. Estrogen deficiency increases osteoclastogenesis up-regulating T cells activity: A key mechanism in osteoporosis. Bone. 2008; 43(1):92–100. [PubMed: 18407820]
12. Rifas L. T-cell cytokine induction of BMP-2 regulates human mesenchymal stromal cell differentiation and mineralization. J Cell Biochem. 2006; 98(4):706–714. [PubMed: 16619272]
13. Rifas L, Arackal S, Weitzmann MN. Inflammatory T cells rapidly induce differentiation of human bone marrow stromal cells into mature osteoblasts. J Cell Biochem. 2003; 88(4):650–659. [PubMed: 12577299]
14. Rifas L, Avioli LV. A novel T cell cytokine stimulates interleukin-6 in human osteoblastic cells. J Bone Miner Res. 1999; 14(7):1096–103. [PubMed: 10404009]

15. Rachon D, Mysliwska J, Suchecka-Rachon K, Wieckiewicz J, Mysliwski A. Effects of oestrogen deprivation on interleukin-6 production by peripheral blood mononuclear cells of postmenopausal women. J Endocrinol. 2002; 172(2):387–395. [PubMed: 11834456]

16. Sugiyama T. Involvement of interleukin-6 and prostaglandin E2 in periarticular osteoporosis of postmenopausal women with rheumatoid arthritis. J Bone Miner Metab. 2001; 19(2):89–96. [PubMed: 11281165]

17. Ota N, Hunt SC, Nakajima T, Suzuki T, Hosoi T, Orimo H, et al. Linkage of interleukin 6 locus to human osteopenia by sibling pair analysis. Hum Genet. 1999; 105(3):253–257. [PubMed: 10987653]

18. Jilka RL, Hangoc G, Girasole G, Passeri G, Williams DC, Abrams JS, et al. Increased osteoclast development after estrogen loss: mediation by interleukin-6. Science. 1992; 257(5066):88–91. [PubMed: 1621100]

19. Manolagas SC, Bellido T, Jilka RL. New insights into the cellular, biochemical, and molecular basis of postmenopausal and senile osteoporosis: roles of IL-6 and gp130. [Review] [49 refs]. Int J Immunopharmacol. 1995; 17(2):109–116. [PubMed: 7657404]

20. Ishihara K, Hirano T. IL-6 in autoimmune disease and chronic inflammatory proliferative disease. Cytokine Growth Factor Rev. 2002; 13(4–5):357. [PubMed: 12220549]

21. Mundy GR, Luben RA, Raisz LG, Oppenheim JJ, Buell DN. Bone-resorbing activity in supernatants from lymphoid cell lines. N Engl J Med. 1974; 290(16):867–871. [PubMed: 4816960]

22. Horton JE, Oppenheim JJ, Mergenhagen SE, Raisz LG. Macrophage-lymphocyte synergy in the production of osteoclast activating factor. J Immunol. 1974; 113(4):1278–1287. [PubMed: 4414541]

23. Chen P, Trummel C, Horton J, Baker JJ, Oppenheim JJ. Production of osteoclast-activating factor by normal human peripheral blood rosetting and nonrosetting lymphocytes. Eur J Immunol. 1976; 6(10):732–6. [PubMed: 797286]

24. Yoneda T, Mundy GR. Monocytes regulate osteoclast-activating factor production by releasing prostaglandins. J Exp Med. 1979; 150(2):338–50. [PubMed: 458377]

25. Weitzmann MN, Pacifici R. Estrogen deficiency and bone loss: an inflammatory tale. J Clin Invest. 2006; 116(5):1186–94. [PubMed: 16670759]

26. Kong YY, Feige U, Sarosi I, Bolon B, Tafuri A, Morony S, et al. Activated T cells regulate bone loss and joint destruction in adjuvant arthritis through osteoprotegerin ligand. Nature. 1999; 402(6759):304–9. [PubMed: 10580503]

27. Weitzmann MN, Cenci S, Rifas L, Brown C, Pacifici R. Interleukin-7 stimulates osteoclast formation by up-regulating the T- cell production of soluble osteoclastogenic cytokines. Blood. 2000; 96(5):1873–8. [PubMed: 10961889]

28. Weitzmann MN, Cenci S, Rifas L, Haug J, Dipersio J, Pacifici R. T cell activation induces human osteoclast formation via receptor activator of nuclear factor kappaB ligand-dependent and -independent mechanisms. J Bone Miner Res. 2001; 16(2):328–337. [PubMed: 11204433]

29. Horwood NJ, Kartsogiannis V, Quinn JM, Romas E, Martin TJ, Gillespie MT. Activated T Lymphocytes Support Osteoclast Formation in Vitro. Biochem Biophys Res Commun. 1999; 265(1):144–150. [PubMed: 10548505]

30. Kotake S, Udagawa N, Hakoda M, Mogi M, Yano K, Tsuda E, et al. Activated human T cells directly induce osteoclastogenesis from human monocytes: possible role of T cells in bone destruction in rheumatoid arthritis patients. Arthritis Rheum. 2001; 44(5):1003–12. [PubMed: 11352231]

31. Rifas L, Arackal S. T cells regulate the expression of matrix metalloproteinase in human osteoblasts via a dual mitogen-activated protein kinase mechanism. Arthritis Rheum. 2003; 48(4): 993–1001. [PubMed: 12687541]

32. Altschul SF, Gish W, Miller W, Myers EW, Lipman DJ. Basic local alignment search tool. J Mol Biol. 1990; 215(3):403–10. [PubMed: 2231712]

33. Donini S, Percudani R, Credali A, Montanini B, Sartori A, Peracchi A. A threonine synthase homolog from a mammalian genome. Biochem Biophys Res Commun. 2006; 350(4):922–8. [PubMed: 17034760]

34. Thierry-Mieg D, Thierry-Mieg J. AceView: a comprehensive cDNA-supported gene and transcripts annotation. Genome Biol. 2006; 7(Suppl 1):S12, 1–14. [PubMed: 16925834]
35. Bendtsen JD, Jensen LJ, Blom N, Von Heijne G, Brunak S. Feature-based prediction of non-classical and leaderless protein secretion. Protein Eng Des Sel. 2004; 17(4):349–56. [PubMed: 15115854]
36. Bendtsen JD, Nielsen H, von Heijne G, Brunak S. Improved prediction of signal peptides: SignalP 3.0. J Mol Biol. 2004; 340(4):783–95. [PubMed: 15223320]
37. Oursler MJ, Bell LV, Clevinger B, Osdoby P. Identification of osteoclast-specific monoclonal antibodies. J Cell Biol. 1985; 100(5):1592–1600. [PubMed: 2580844]
38. Matsuo K, Galson DL, Zhao C, Peng L, Laplace C, Wang KZ, et al. Nuclear factor of activated T-cells (NFAT) rescues osteoclastogenesis in precursors lacking c-Fos. J Biol Chem. 2004; 279(25): 26475–80. [PubMed: 15073183]
39. Takayanagi H. The role of NFAT in osteoclast formation. Ann N Y Acad Sci. 2007; 1116:227–37. [PubMed: 18083930]
40. Skoumal M, Kolarz G, Haberhauer G, Woloszczuk W, Hawa G, Klingler A. Osteoprotegerin and the receptor activator of NF-kappa B ligand in the serum and synovial fluid. A comparison of patients with longstanding rheumatoid arthritis and osteoarthritis. Rheumatol Int. 2005; 26(1):63–9. [PubMed: 15889303]
41. Vanderborght A, Linsen L, Thewissen M, Geusens P, Raus J, Stinissen P. Osteoprotegerin and receptor activator of nuclear factor-kappaB ligand mRNA expression in patients with rheumatoid arthritis and healthy controls. J Rheumatol. 2004; 31(8):1483–1490. [PubMed: 15290725]
42. Zhang YH, Heulsmann A, Tondravi MM, Mukherjee A, Abu-Amer Y. Tumor Necrosis Factor-alpha (TNF) Stimulates RANKL-induced Osteoclastogenesis via Coupling of TNF Type 1 Receptor and RANK Signaling Pathways. J Biol Chem. 2001; 276(1):563–568. [PubMed: 11032840]
43. Kobayashi K, Takahashi N, Jimi E, Udagawa N, Takami M, Kotake S, et al. Tumor Necrosis Factor alpha Stimulates Osteoclast Differentiation by a Mechanism Independent of the ODF/RANKL-RANK Interaction. J Exp Med. 2000; 191(2):275–286. [PubMed: 10637272]
44. Wong BR, Josien R, Lee SY, Sauter B, Li HL, Steinman RM, et al. TRANCE (tumor necrosis factor [TNF]-related activation-induced cytokine), a new TNF family member predominantly expressed in T cells, is a dendritic cell-specific survival factor. J Exp Med. 1997; 186(12):2075–80. [PubMed: 9396779]
45. Hashizume M, Hayakawa N, Mihara M. IL-6 trans-signalling directly induces RANKL on fibroblast-like synovial cells and is involved in RANKL induction by TNF-alpha and IL-17. Rheumatology (Oxford). 2008; 47(11):1635–40. [PubMed: 18786965]
46. Hofbauer LC, Heufelder AE. Intercellular chatter: osteoblasts, osteoclasts and interleukin 6. Eur J Endocrinol. 1996; 134(4):425–426. [PubMed: 8640290]
47. Wong PK, Quinn JM, Sims NA, van NA, Campbell IK, Wicks IP. Interleukin-6 modulates production of T lymphocyte-derived cytokines in antigen-induced arthritis and drives inflammation-induced osteoclastogenesis. Arthritis Rheum. 2006; 54(1):158–168. [PubMed: 16385511]

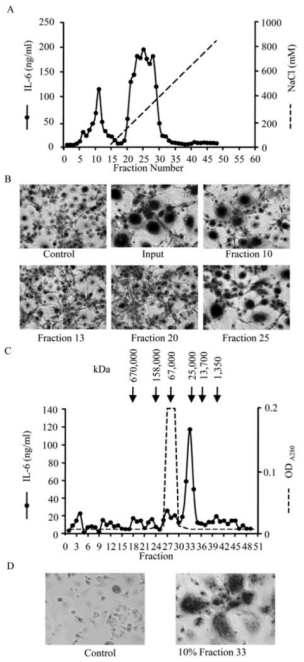

Figure 1.

Induction of IL-6 and TRAP+ osteoclast-like cells by fractionated activated T cell conditioned medium. DEAE Sepharose column chromatography with peak fractions assayed for: **(A)** IL-6 (Left Y-axis) or **(B)** osteoclastogenic activity. Multinucleated TRAP+ cells represent osteoclasts. Control=untreated cells; Input= unfractionated T cell conditioned medium. **(C)** Superdex-200 fractionation of the major DEAE-sepharose peak (panel A) reveals a single peak containing both **(C)** IL-6 activity and **(D)** osteoclastogenic activity.

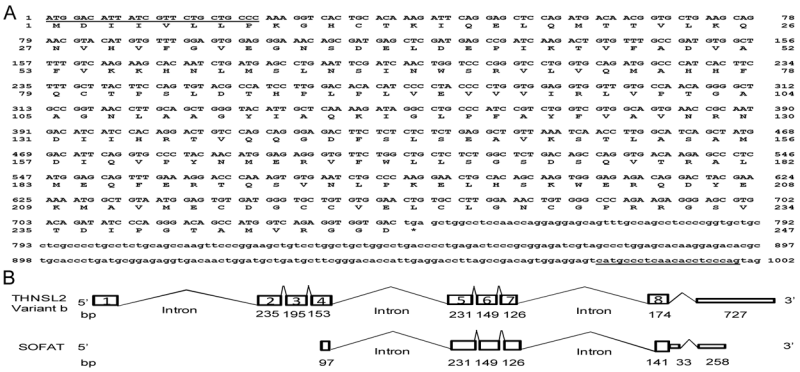

Figure 2.

Nucleotide sequence, protein translation and gene structure of human SOFAT. **(A)** hSOFAT was cloned based on alignment of amino acid sequence derived from mass spectroscopy with hypothetical protein FLJ10916 and nucleotide sequence thus deduced. Position of 3′ and 5′ RT-PCR primers are underlined. The nucleotide sequence of hSOFAT was determined by sequencing of cDNA reverse transcribed from activated T cell total RNA and the protein sequence rederived there from. hSOFAT comprises 247 amino acids. A larger version of Part A is contained in Supplemental Figure 6. **(B)** Representation of how SOFAT is generated from THNSL2, using splice variant “b” (see Supplemental Figure 2) as the reference sequence. Exons shown as numbered black boxes, introns as lines (not too scale), and untranslated regions as narrow open bars. SOFAT shows highest homology to splice variant “b”, and comprises the last 97 bp of exon 4 joined to exons 5, 6, and 7, plus the first 141 bp of exon 8. An additional 33 bp of 3′UTR sequence and at least 258 bp of non coding UTR derived from an unused exon 9 is contained within the boundaries of the 3′ primer.

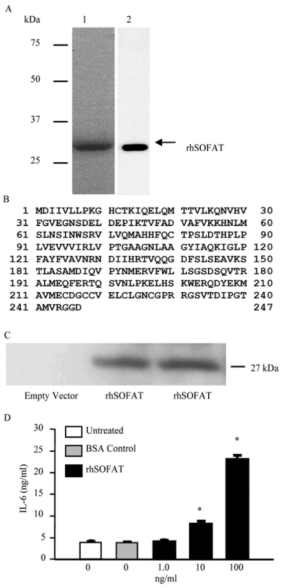

Figure 3.

Expression of recombinant SOFAT, protein translation and IL-6 inducing activity. **(A)** E. coli expressed rhSOFAT was resolved by SDS-PAGE and Coomassie Blue stained (Lane 1), and immunoprobed with anti-polyhistidine antibody (Lane 2). **(B)** Protein identity was verified by MS sequencing. **(C)** To examine secretion, SOFAT was immunoprecipitated from CHO cell supernatant and assayed on Western blot by anti-polyhistidine antibody. Replicate assays of rhSOFAT are shown. **(D)** ELISA assay of rhSOFAT induced IL-6 production in osteoblasts. Data represent mean ± S.E.M. of triplicate cultures. * = $p < 0.001$ (One Way ANOVA,) relative to untreated cells (Untreated) and Bovine Serum Albumin (BSA) treated cell controls.

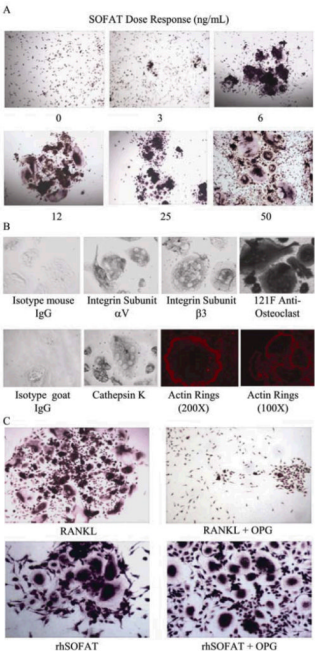

Figure 4.

Generation and characterization of human osteoclasts by rhSOFAT. **(A)** Dose Response: Human monocytes were cultured with rhSOFAT for 10 days and stained for TRAP. Magnification = 100×. **(B)** Monocytes were cultured with rhSOFAT (100 ng/mL) for 7 days and immunostained with mouse IgG antibodies against αV and β3 integrin subunits, and the anti-osteoclast antibody 121F, or with goat IgG antibodies against cathepsin K or with the relevant mouse or goat IgG isotype controls. Magnification = 100×. Actin ring formation was visualized under fluorescence microscopy. Magnification = 100× or 200× as indicated. **(C)** Human monocytes were cultured with either 25 ng/mL RANKL or 100 ng/mL SOFAT ± 200 fold excess OPG for 10 days and stained for TRAP. Magnification = 100×.

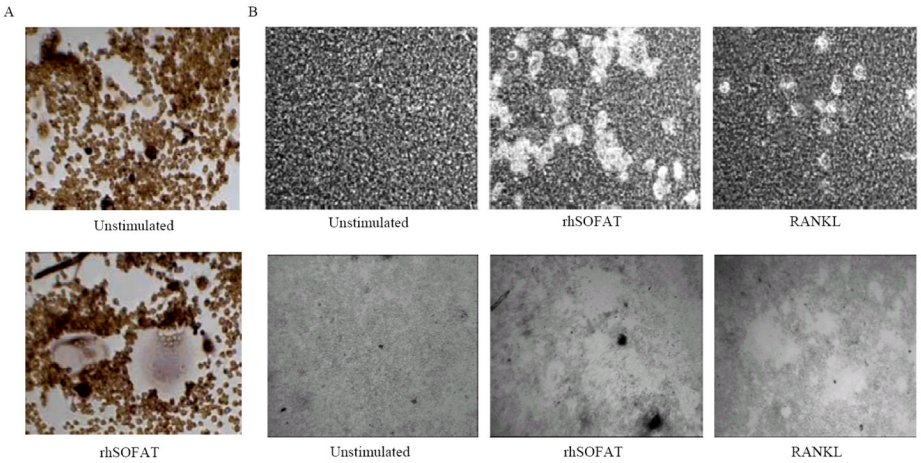

Figure 5.

rhSOFAT-induces functional osteoclasts by mouse RAW264.7 cells. **(A)** Mouse RAW264.7 cells were treated with rhSOFAT (100 ng/mL) for 5 days and TRAP stained. Photographed at 100× magnification. **(B)** To test osteoclast activity RAW264.7 cells were cultured untreated on BioCoat, or treated with rhSOFAT (100 ng/mL) or RANKL (60 ng/mL) for 10 days. Lower panel shows bright field microscopy of pits at 100× magnification. Top panel shows phase contrast microscopy of resorption pits at 200 × magnification.

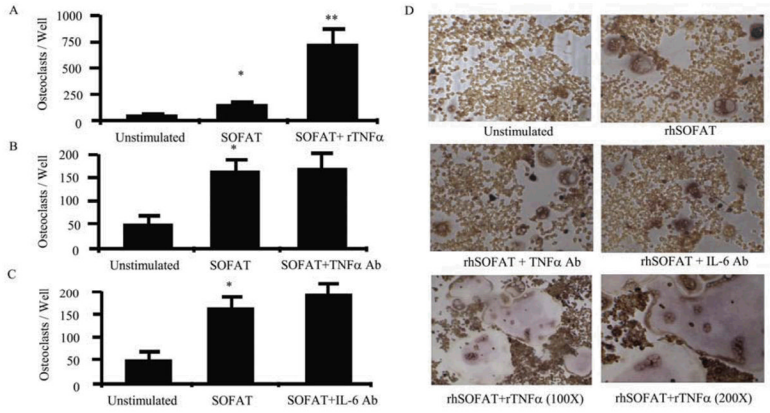

Figure 6.

SOFAT requires neither TNFα nor IL-6 for osteoclast formation however; TNFα amplifies rhSOFAT induced osteoclastogenesis. RAW264.7 cells were cultured with rhSOFAT (100 ng/mL) ± **(A)** TNFα (10 ng/mL); **(B)** neutralizing anti-TNFα antibody (20 μg/mL); or **(C)** anti-IL-6 antibody (20 μg/mL). After 5 days TRAP+ multinucleated cells were quantitated under light microscopy. *<0.001 vs Unstimulated; **<0.001 vs SOFAT (1-way ANOVA (Tukey-Kramer). Data represent mean ± SD of 6 replicate wells. **(D)** A representative field for each experiment (**A**, **B**, and **C**). Magnification = 100 × or 200 ×. In a pilot experiment, TNFα, and anti-TNFα and anti-IL-6 were observed to have no effect on RAW264.7 cells in the absence of SOFAT. We also verified that the TNFα antibody used, neutralized 10 ng/mL of rTNFα on osteoclast formation. (Data not shown).